Chemical Science

EDGE ARTICLE

View Article Online
View Journal | View Issue

Cite this: *Chem. Sci.*, 2017, **8**, 5746

Mono-*N*-protected amino acid ligands stabilize dimeric palladium(II) complexes of importance to C–H functionalization†

Joseph J. Gair,[a] Brandon E. Haines,[b] Alexander S. Filatov,[a] Djamaladdin G. Musaev*[b] and Jared C. Lewis*[a]

Mono-protected amino acid (MPAA) ligands are used in a number of Pd-catalyzed C–H functionalization reactions. MPAAs have been proposed to bind to Pd(II) *via* κ^2-(*N*,*O*) coordination, but such binding has not yet been experimentally validated. Herein, we report the synthesis and detailed characterization of a series of MPAA complexes prepared *via* cyclopalladation of dimethylbenzylamine in the presence of MPAAs. The isolated complexes exist as μ-carboxylato (MPAA) bridged dimers and feature potential M–M cooperativity and secondary sphere hydrogen bonding. Selective MPAA coordination and relay of stereochemistry, previously suggested to uniquely result from κ^2-(*N*,*O*) MPAA coordination, are both observed. The isolated MPAA complexes undergo C–C and C–X (X = Cl, Br, I) bond formation when treated with electrophiles used for catalytic C–H functionalization. Stoichiometric iodination of MPAA palladacycles was found to proceed *via* a dinuclear palladium species with one equivalent of iodine in the rate limiting transition structure, and the isolated complexes also served as viable precatalysts for catalytic C–H functionalization. Together, these results provide a number of insights into the reactivity of Pd-MPAA complexes relevant to C–H bond functionalization.

Received 14th April 2017
Accepted 15th June 2017

DOI: 10.1039/c7sc01674c

rsc.li/chemical-science

Introduction

One of the foremost challenges in transition metal catalyzed C–H functionalization has been the development of catalysts that selectively modify one C–H bond in the presence of others with similar steric and electronic properties.[1–6] Palladium catalyzed transformations that exploit the ability of Lewis basic functional groups within a substrate to coordinate to the metal catalyst and thus confer site selectivity to C–H bond cleavage (activation) have long proven particularly useful in this regard.[7–9] In combination with this approach, mono-*N*-protected amino acid (MPAA) ligands have been found to accelerate[10,11] and impart enantioselectivity[12–17] to several Pd(II)-catalyzed C–H functionalization reactions.[18]

Numerous approaches, including DFT calculations,[19–23] mass spectrometry,[24,25] and steady state kinetics[10,26] have been used to investigate the mechanism(s) by which MPAA ligands affect Pd(II)-catalyzed C–H functionalization. These studies have concluded that MPAA-promoted, Pd(II)-catalyzed C–H bond functionalization proceeds *via* a N–H cleavage and subsequent C–H activation mechanism.[21] The proposed active catalyst is generated by κ^2-(*N*,*O*) coordination of MPAA to Pd(II) (Chart 1) followed by deprotonation of the *N*-protected amide. Concerted metallation-deprotonation (CMD)[27–31] of the substrate C–H bond by either the *N*-protecting group[25] of the MPAA ligand or an external base[19] could then occur. κ^2-(*N*,*O*) binding of the MPAA ligand is thought to enforce a rigid structure capable of relaying chirality from the MPAA to a prochiral substrate in the CMD transition state.[24] With the development of this mechanistic paradigm, it has become widely accepted that the active catalysts are monomeric κ^2-(*N*,*O*) Pd(II)MPAA complexes.

Notably, however, no Pd(II)MPAA intermediates in these reactions have been rigorously characterized in solution or by X-ray diffraction. To shed light on the nature of MPAA coordination to Pd(II) and to understand the impact that MPAA coordination has on the nuclearity and stoichiometric reactivity of these complexes, we sought to isolate and characterize Pd(II)

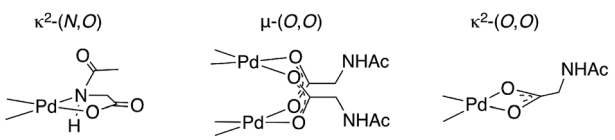

Chart 1 Three potential modes for coordination of the MPAA *N*-acetylglycine to Pd(II).

[a]*Department of Chemistry, The University of Chicago, Chicago, Illinois, 60637, USA. E-mail: jaredlewis@uchicago.edu*

[b]*Cherry L. Emerson Center for Scientific Computation, Emory University, 1515 Dickey Drive, Atlanta, Georgia 30322, USA. E-mail: dmusaev@emory.edu*

† Electronic supplementary information (ESI) available: Experimental procedures, analytical and spectral characterization data for all new compounds, and crystallographic information files (CIF) for compounds **2**, **6a–c**, **15**, **16**, **17**, S1.4, and S5.1. CCDC 1544213–1544221. For ESI and crystallographic data in CIF or other electronic format see DOI: 10.1039/c7sc01674c

MPAA complexes analogous to those invoked for catalysis. Such complexes would also serve as models to specifically probe and understand individual steps of proposed catalytic cycles and guide the design of new and more effective ligands for C–H functionalization catalysis.

Results and discussion

Synthesis of MPAA complexes *via* ligand exchange

Putative κ^2-(*N*,*O*) binding of MPAA ligands to Pd(II) during catalytic C–H functionalization was first proposed[17] in the literature based on the previously reported[32] synthesis of **1**, Pd(dmba)(NAc-Gly) (Fig. 1a, dmba = *N*,*N*-dimethylbenzylamine, NAc-Gly = *N*-acetyl-glycine). Indeed, we obtained a good yield (71%) of a complex consistent with the ^{1}H and ^{13}C NMR data reported for **1** by following this procedure. The κ^2-(*N*,*O*) MPAA coordination in **1** was originally assigned based on analogy to the corresponding unprotected glycine complex.[32,33] To gain further confidence in this assignment, we determined the structure of the isolated product by single-crystal X-ray analysis. The structure observed in the solid state is the μ^2-(*O*,*O*) MPAA-bridged dimer complex **2** (Fig. 1c) instead of the reported κ^2-(*N*,*O*) complex **1**.

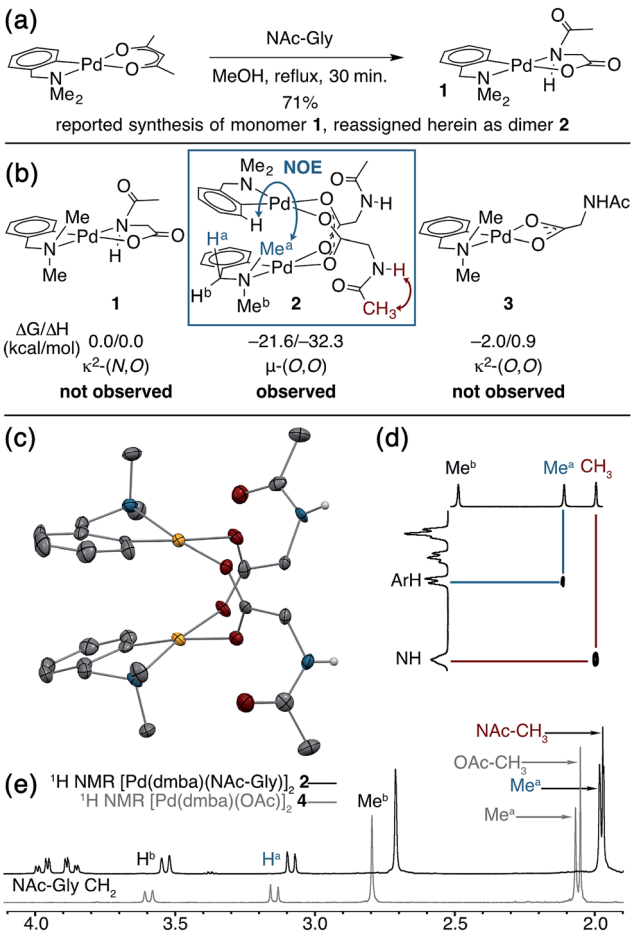

Fig. 1 (a) Previously reported synthesis of **1**, which is herein reassigned as complex **2**. (b) Relative calculated energies (Δ*G*/Δ*H*) of **1**, **2**, and **3** with observed NOEs noted on **2**; (c) ORTEP diagram of **2** with 50% ellipsoids; in structures throughout yellow = Pd, red = O, blue = N, grey = C, white = H, and green = halogen; (d) portion of ^{1}H NOESY spectrum with diagnostic cross peaks; (e) overlaid ^{1}H NMR spectra of MPAA complex **2** with acetate complex **4** offset by 0.1 ppm for clarity.

To address the possibility that this dimer may only exist in the solid state, a solution of **2** was analyzed by ^{1}H NMR, NOESY, and ESI-MS—all of which are consistent with a dimeric MPAA-bridged palladium complex. An initial indication of a dimeric complex in solution is the large upfield shift in one of the inequivalent benzylic resonances (H^a) and *N*-methyl resonances (Me^a) relative to the precursors [Pd(dmba)(Cl)]$_2$ and Pd(dmba)(acac) (acac = acetylacetonate) (Fig. 1b and e). This large upfield shift is consistent with proximity to the ring current of an aromatic π-system—as one would expect for the carboxylate bridged dimer **2**—and is strikingly similar to the ^{1}H NMR of known acetate bridged dimer **4** [Pd(dmba)(OAc)]$_2$ (Fig. 1e).[34–36] The most direct evidence for the existence of **2** as a dimer in solution is the presence of an NOE between the aromatic C–H *ortho* to palladium with the upfield NMe^a and while the downfield resonance NMe^b has no such NOE (Fig. 1d).

DFT calculations[37] were conducted to gain further insight into the stability of the dimeric structure of **2**. Good agreement between the calculated and crystal structures of **2** is observed; for example, the Pd–Pd distances in the two structures are 2.95 and 2.99 Å, respectively (see ESI† for full structural analysis). Moreover, the free energy/enthalpy of dimerization (ΔG_{dimer}/ΔH_{dimer}) for **2** (*i.e.* energy of the reaction 2(**1**) → **2**) is calculated to be −21.6/−32.3 kcal mol^{-1} (Fig. 1b). This finding shows that the dimeric structure **2** is significantly more stable than that of two putative monomers (**1**). Calculations also indicate that the κ^2-(*N*,*O*) coordination mode of NAc-Gly in **1** is less stable than the κ^2-(*O*,*O*) binding mode (**3**) by 2.0 kcal mol^{-1}, suggesting that the proposed κ^2-(*N*,*O*) coordination mode may not be the most stable monomer complex. We also located a μ-(*N*,*O*) dimer structure with dmba and NAc-Gly, **2**-μ-(*N*,*O*), that is higher in energy than **2** by 16.0 kcal mol^{-1}. These results show, for the first time, that widely used MPAA ligands can stabilize dimeric, μ-(*O*,*O*) carboxylate-bridged Pd(II)MPAA complexes directly analogous to widely-studied acetate-bridged palladacycles.[38–43]

Synthesis of MPAA complexes *via* C–H activation

To determine if **2** could also be prepared *via* cyclopalladation of dmba in the presence of MPAA, an equimolar mixture of palladium acetate, dmba, and NAc-Gly was stirred at room temperature in methanol. Analysis of the crude reaction mixture revealed **2** as the major product despite the presence of a 2 : 1 excess of acetate : MPAA, indicating selective coordination of MPAA over acetate. Complete conversion of dmba was observed overnight, and a 57% isolated yield of **2** was obtained after crystallization. These conditions were used to prepare MPAA-bridged complexes **6a–d** (NAc-Gly, NAc-Ala, NAc-Leu, NAc-Ile) from trifluoromethyl dmba derivative **5a** (F_3C-dmba) in 62–91% yield by ^{19}F NMR (Scheme 1).

DFT calculations performed for **6a–d** and their acetate-bridged analogue, **9**, are consistent with these experimental findings. In all cases, the formation of carboxylate-bridged

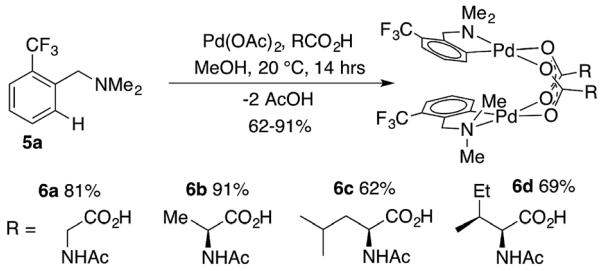

Scheme 1 Synthesis and ^{19}F NMR yields of carboxylate bridged F_3C-dmba dimers **6a–d**.

dimers, [(dmba)Pd(MPAA)]$_2$, from separated monomers is calculated to be highly exergonic: $\Delta G_{dimer}/\Delta H_{dimer}$ = −18.5/−35.9, −18.5/−36.7, −21.0/−39.0, −21.5/−39.6 and −17.3/−33.1 kcal mol^{-1} for **6a**, **6b**, **6c**, **6d** and **9**, respectively. These computational data demonstrate that all studied MPAAs form more stable dimeric complexes than their acetate analogs. Furthermore, the stability of [(dmba)Pd(MPAA)]$_2$ relative to the corresponding monomers increases with increasing size of the MPAA ligand side chain (*i.e.*, **6c**/**6d** > **6a**/**6b**). Similar to our previous findings for acetate-bridged Pd(II) complexes, however, it is expected that the stability of MPAA-bridged complexes will depend on the nature of substrate directing group, MPAA, and environment (solvent, additives, *etc.*).[44]

Characterization of dimeric Pd(II)MPAA complexes

Single crystal X-ray diffraction studies of **6b–d** confirm that each of these complexes exists as a carboxylate-bridged dimer in the solid state. However, detailed mechanistic studies are not possible without an understanding of structure in solution: though solid state structures can provide insight, solution structures and aggregation states must be determined independently.[45,46] Pulse gradient spin-echo (PGSE) experiments were conducted to assess the nuclearity of the MPAA complexes in solution.[47,48] The molecular volume of the monomeric acac complex **7** was benchmarked at 1.0 and the dimeric acetate and chloride bridged complexes (**8** and **9**) gave molecular volumes of 1.9 and 2.4 relative to **7**, indicating the ability of PGSE experiments to differentiate monomeric from dimeric Pd(dmba) complexes (Chart 2). Under the same conditions, the MPAA complexes **6a–d** all gave relative molecular radii greater than the dimeric control complexes (3.9–4.8) consistent with dimeric MPAA complexes in solution.

The dimeric nature of complexes **6a–d** in solution is further supported by their ^{1}H NMR and NOESY spectra, which display the same diagnostic features as the acetate bridged complexes **4** and **9** (Fig. 1e and Chart 2, respectively). Specifically, upfield shifts due to magnetic anisotropy and NOE cross peaks with upfield-shifted resonances were observed. Full characterization for **6a–d** is provided in the ESI† (^{1}H, ^{13}C{^{1}H}, ^{19}F, HMQC, COSY, and NOESY).

A noteworthy feature of carboxylate bridged palladacycles is the chirality of the stacked, square planar coordination spheres (Chart 3). As expected for an achiral ligand, all of the NAc-Gly

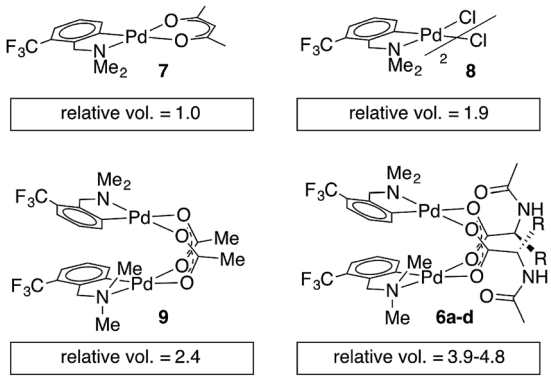

Chart 2 Relative molecular volumes approximated from diffusion coefficients obtained by pulse gradient spin-echo NMR.

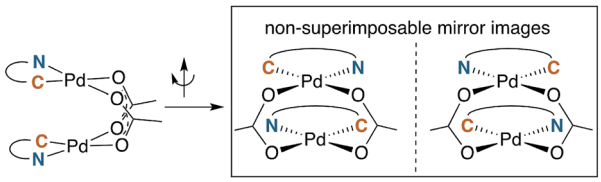

Chart 3 Chirality of carboxylated bridged palladacycles.

complexes crystallize as racemic mixtures with both enantiomers present in the unit cell. When an additional stereogenic unit is introduced to the MPAA (**6b–d**), the chirality of the complex gives rise to two diastereomers, which are present in an approximately equal ratio for **6b–d** and are differentiable by NMR as illustrated in Fig. 2. It is interesting to note that, despite a nearly 10 Å separation of the CF_3 substituents and the stereogenic centers of the MPAA ligands, the extent of diastereotopic differentiation of ^{19}F NMR appears to be correlated with the size of the MPAA side chain ($\Delta\delta$ = 4.5, 15, and 26 Hz for R = Me (**6b**), *iso*-Bu (**6c**), and *sec*-Bu (**6d**)).

Assessing monomer dimer equilibrium

To address the possibility that other species (*e.g.*, κ^2-(*N*,*O*) monomer) may be in equilibrium with the observed MPAA-bridged dimers, a crossover experiment was conducted which revealed rapid equilibration of homodimers to a statistical mixture of hetero and homodimers (Scheme 2 and ESI S1.5†).[43]

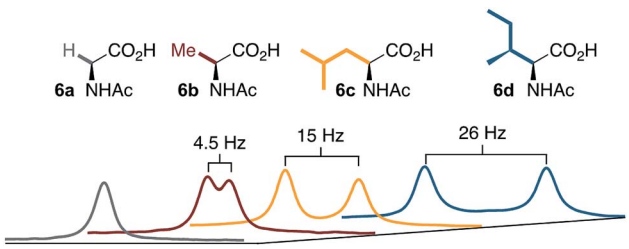

Fig. 2 ^{19}F NMR of **6a–d** show correlation between diastereotopic differentiation and size of MPAA side chain.

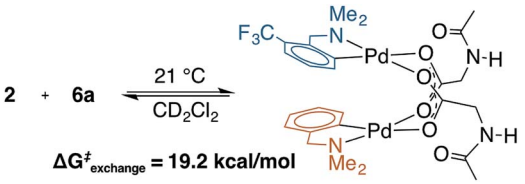

Scheme 2 Crossover experiment with MPAA bridged dimers **2** and **6a** reveals rapid exchange.

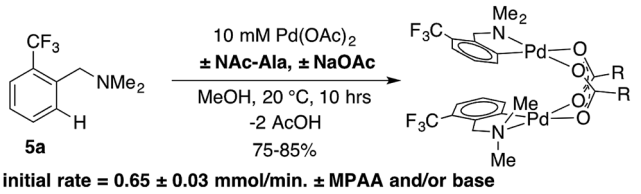

Scheme 3 MPAA and carboxylate bases showed no effect on the rate of cyclopalladation of **5a**.

Rapid crossover at room temperature is consistent with a small equilibrium concentration of monomeric MPAA complex capable of rapidly recombining with other free monomers in solution. This rapid equilibrium was further assessed by ^{19}F EXSY experiments which revealed $\Delta G^{\ddagger}_{\text{exchange}} = 19.2$ kcal mol^{-1} at 21 °C.[49] The observed $\Delta G^{\ddagger}_{\text{exchange}}$ is comparable to the calculated ΔG_{dimer} of **6a** (18.5 kcal mol^{-1}) and thus compatible with an exchange pathway proceeding through high energy monomeric intermediates (see ESI S1.5† for ^{19}F EXSY).

The rapid exchange of homodimers to equilibrium mixtures of homo and heterodimers enabled analysis by the method of continuous variation (MCV) which has proven especially powerful for characterizing the structure and aggregation state of complex mixtures in solution.[45,46,50] This approach confirmed the dimeric nature of **2** and **6a** in solution by revealing a characteristic statistical ensemble of dimers (see ESI S1.5† for Job plot).[50] Complexes **6a** and **6b** were further characterized by variable temperature ^{1}H NMR (233–353 K), variable concentration ^{19}F NMR (3–39 mM), and variable concentration UV-vis (0.02–0.5 mM) to further assess the presence of the putative monomeric species involved in the equilibrium shown in Scheme 2. Across this range of conditions, there was no observable monomer or any other species in equilibrium with the characterized dimeric (MPAA)Pd-complexes. Attempts to observe monomeric (MPAA)Pd-complexes by trapping with excess of amine substrate revealed no change in the ^{1}H and ^{19}F spectra of **6a** with up to 100 equivalents of **5a** (ESI S1.4†). Collectively, these results as well as the DFT-calculated dimerization energies are consistent with the existence of high energy monomer complexes in rapid equilibrium with the observed MPAA-bridged dimer complexes.

Effect of MPAA on rate of cyclopalladation

As noted above, C–H activation of dmba with palladium acetate gives selective formation of MPAA-bridged over acetate-bridged di-palladium products, the later of which have been extensively characterized in stoichiometric studies and as catalytic intermediates.[38–43]

This selectivity could result from more favorable binding of MPAA relative to acetate or faster cyclometallation by a Pd/MPAA species relative to Pd/OAc. Cyclopalladation of CF_3-dmba to afford discrete MPAA complexes (**6a–d**) provides a unique model system to study the impact of MPAA on cyclopalladation rates. Initial rates for the reaction shown in Scheme 3 were similar in the presence and absence of NAc-Ala and sodium acetate (NaOAc). These results suggest that kinetic effects are not responsible for the selective coordination of MPAA over acetate in compounds **6a–d**. Previous studies have suggested that observed rate enhancements in MPAA catalyzed C–H functionalization are the result of MPAA ligands lowering the barrier to C–H cleavage. However, MPAA accelerated C–H cleavage has not yet been directly confirmed in stoichiometric reactions, and in the system studied here, a rate effect does not account for selective MPAA coordination.

Pd(II)-MPAA binding affinity

To determine whether thermodynamic factors are responsible for selective MPAA coordination during the formation of **6a–d**, carboxylate exchange reactions were conducted using AcOH, NAc-Gly, NAc-Ala, and NAc-Ile (Scheme 4). In forward and reverse reactions involving NAc-Gly, an equilibrium mixture containing approximately 5% acetate-bridged complex **9** was observed.[51] In contrast, when **9** was equilibrated with NAc-Ala and NAc-Ile, the bulkier MPAA's drove the equilibrium to <1% complex **9**. Poor solubility of NAc-Gly and overlapping chemical shifts of NAc-Ala and NAc-Ile complexes precluded quantitative evaluation of the binding affinities of MPAAs and acetate. Qualitatively however, our experiments show that NAc-Gly, NAc-Ala, and NAc-Ile selectively displace acetate and suggest that NAc-Ala and NAc-Ile have a greater binding affinity than NAc-Gly (see ESI S1.8† for ^{1}H and ^{19}F NMR of MPAA/OAc equilibrium mixtures). Thus, while these are structurally similar to acetate bridged dimers, differential binding strength leads to selective coordination of MPAAs, which can carry stereochemical information.

To better understand bridging carboxylate binding affinity, we extended our DFT studies to examine ligand exchange equilibria ($\Delta G_L/\Delta H_L$) between acetate and MPAA ligands as defined by the equation: **9** + 2 MPAA → **6a**/**6b**/**6d** + 2 AcOH

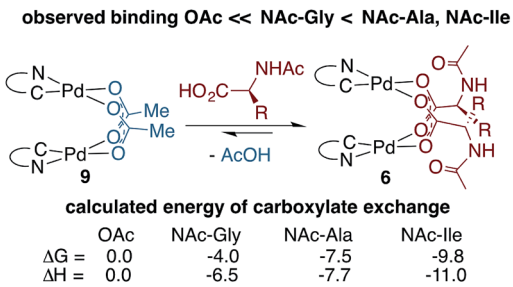

Scheme 4 Competitive carboxylate binding equilibria.

(Scheme 4).[52] The ligand exchange equilibrium was found to favor coordination of the MPAA ligands in the dimer complex, where $\Delta G_L/\Delta H_L = -4.0/-6.5$, $-7.5/-7.7$ and $-9.8/-11.0$ kcal mol^{-1} for **6a**, **6b**, and **6d**, respectively. The thermodynamic preference for MPAA binding relative to acetate is consistent with the results of a previous study on carboxylate-bridged palladium(II) dimers, in which we found that electron-withdrawing groups on bridging carboxylates stabilize the dimer relative to separated monomers by increasing interaction energy between the Pd-center and ligands (*i.e. via* the Pd–OCO bonding motif) (see Table S2.3 in the ESI† for charge analysis).[44] Thus, both experimental and computational results suggest bridging carboxylate binding affinity follows the trend acetate < NAc-Gly < NAc-Ala, NAc-Ile.

Substrate scope of C–H activation

To assess whether substrates used in C–H functionalization reactions catalyzed by Pd(II)/MPAA mixtures can form dimeric complexes analogous to **6a–d**, 1 mM methanol solutions of $Pd(OAc)_2$, NAc-Ala, and substrate were analyzed by ESI-MS after 30 minutes of mixing (Fig. 3a).[17,53,54] The substrate dmba (in **11**) was studied to confirm that reaction mixtures afforded similar mass spectra to the isolated complex **2**. The substrates 2-pyridyl-diphenylmethane[17] (in **12**) and dimethylamino-ferrocenyl-methane[53,54] (in **13**) were also evaluated because both have been used in enantioselective Pd(II)/MPAA catalyzed C–H functionalization. Moreover, the former was the subject of computational,[21] synthetic,[21] and mass spectrometry[24] experiments aimed at understanding the impact of MPAA ligands on catalysis, and the latter was used in stoichiometric enantioselective cyclopalladation reactions with MPAA additives.[55–58] Thus, while these substrates cannot, of course, represent the full scope Pd(II)/MPAA catalyzed C–H functionalization due to the sensitivity of these reactions to different directing groups,[59] they are structurally similar to dmba, which we have studied in depth, and both have been used for stoichiometric model studies[21,24,55–58] and catalysis.[17,53,54]

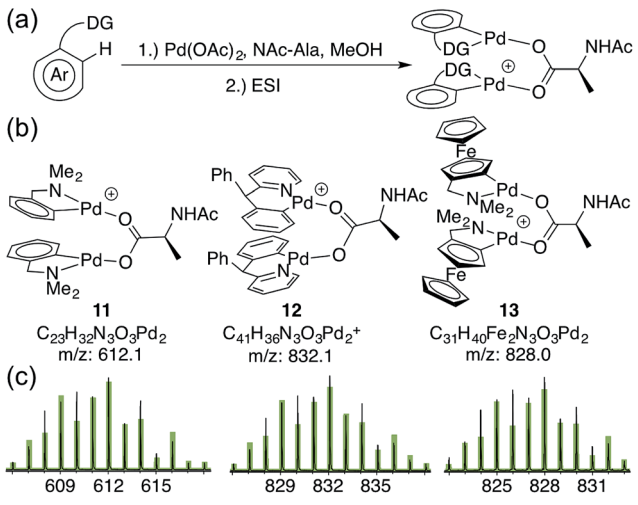

Fig. 3 (a) Reaction conditions to generate MPAA complexes for analysis by ESI-MS; (b) ions for di-palladium MPAA complexes (1 MPAA) (c) observed isotope patterns for ions **11–13** (black) and overlaid theoretical isotope patterns (green) from ESI-MS analysis of reactions in (a).[62]

As expected, the di-palladium ion **11** (with dmba substrate) was observed. While ions consistent with monomeric cyclopalladated (MPAA)Pd-complexes were previously reported for 2-pyridyl-diphenylmethane,[24] we observe ions consistent with both monomeric and dimeric Pd species (**12**) for this substrate[17,60] and for dimethylamino-ferrocenyl-methane[53,54,61] (**13**) (Fig. 3). The observed di-palladium ions are analogous to those observed in the MS of isolated, characterized carboxylate-bridged dimers **2**, **4**, **6a–d** and **9**. Moreover, di-palladium ions **11–13** had a higher intensity than those corresponding MPAA to monomeric complexes. For all three substrates, the palladium-containing ion with the greatest intensity is the cyclopalladated substrate with no ancillary ligands (or a fragment thereof) (see Sections S4.1, S4.2 and S4.3 in the Section S3 in the ESI† for full spectra of **11**, **12**, and **13** respectively).

Given the observation of ions consistent with di-palladium substrate complexes by MS, we sought to determine whether di-palladium complexes are also present in the absence of substrate.[63] While a previous report[25] noted the monomeric species $Pd(MPAA)^+$ under such conditions, we found that 2 mM acetonitrile solutions of $Pd(OAc)_2$ and MPAA (NAc-Gly, NAc-Ala, and NAc-Leu) contain an ion corresponding to the dimeric complex $Pd_2(MPAA)_2^+$ in addition to $Pd(MPAA)^+$ in ratios dependent on fragmentor voltage (see Sections 4.4–4.6 in the ESI† for labeled spectra from 50–230 V). These results suggest that MPAA-bridged di-palladium species can form both in the absence and presence of multiple substrates used in enantioselective C–H functionalization under conditions similar to those used in the preparation of dimeric MPAA-bridged palladacycles **6a–d**.

We have also calculated the $\Delta G_{dimer}/\Delta H_{dimer}$ values for cyclopalladated carboxylate bridged Pd/MPAA species with 2-pyridyl-diphenylmethane[60] and 2-benzylpyridine[64] substrates, as well as with acetonitrile (*i.e.*, no substrate). In all cases, we find that the dimer is favored over the separated two monomers (see Section S2.4 in the ESI† for full details). As in our previous study, these calculations show that the nature of substrate can have a large impact on the thermodynamic stability of dimeric complexes.[44] For example, calculations show that the additional phenyl substituent of 2-pyridyl-diphenylmethane stabilizes the corresponding cyclopalladated dimer complex relative to that derived from 2-benzylpyridine. The presented calculations are consistent with the experimental data showing that MPAA-bridged dimeric complexes can form with a wide range of substrates relevant for C–H functionalization.

Reactivity of MPAA complexes toward electrophiles

The facile formation of dimeric Pd(II)MPAA complexes **2** and **6a–d**, along with the observation by MS and the calculated energies of analogous complexes with substrates used in catalysis, suggests that MPAA-bridged complexes could form under conditions relevant to catalytic C–H functionalization. The reactivity of **2** and **6b** toward electrophiles used in MPAA-

facilitated C–H functionalization was therefore assessed. Both complexes underwent reaction with Michael acceptors,[10,65] hypervalent iodine oxidants,[66] and elemental halogens[12,67] to give C–C and C–X (X = Cl, Br, I) bond formation as illustrated in Scheme 5.[68]

To determine whether **6b** reacts with electrophiles as a dimer or perhaps as a putative monomeric species, a kinetic analysis was performed of the reaction of **6b** with I_2 (though **6b** may react differently with other electrophiles). Initial control experiments revealed that iodination of **6b** in the presence of increasing, catalytic amounts of exogenous iodide (0.033–0.53 equiv., Bu_4NI) exhibits saturation behavior (Fig. 4b). Thus, to avoid interference from iodide that may be generated over the course of the iodination reaction, the order with respect to iodine was determined in the presence of a saturating concentration of Bu_4NI (53 mol%). Under these conditions, initial rate analysis indicated that the reaction was first order in iodine from 3–39 mM (Fig. 4c). Under pseudo first order conditions, the disappearance of **6b** could be fit using a single exponential function indicating first order kinetics (Fig. 4d). These results, in the presence of catalytic exogenous iodide, are consistent with a reaction of iodine with the dimer **6b** in the rate limiting transition structure, rather than reaction at a monomeric intermediate. Additional data and discussion of iodination in the absence of exogenous iodide are presented in the ESI† (see Section S1.14 for Experimental data and S2.6† for computational analysis).

Observation of C–H activation from MPAA palladacycles

While studying the reactivity of Pd(II)/MPAA complexes toward electrophiles, we found that cyclopalladated substrates with a C–H bond *ortho* to the directing group can undergo subsequent C–H activation chemistry. This reactivity affords a unique opportunity to study C–H activation in MPAA complexes with well-defined, di-palladium reactants and products. For example, combining **2** and iodobenzene dichloride led to the formation of chlorinated Pd(II)MPAA complexes **15a** and **15b**

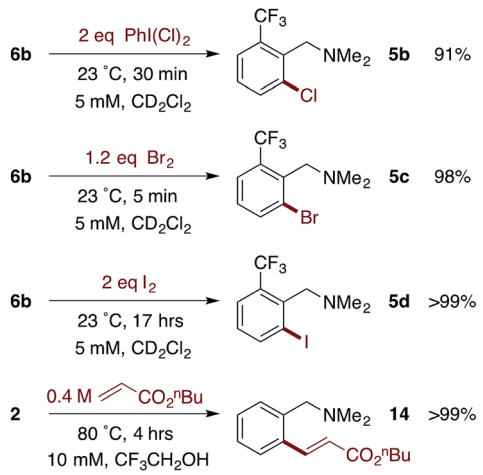

Scheme 5 Representative reactions of cyclopalladated MPAA complexes with electrophiles.

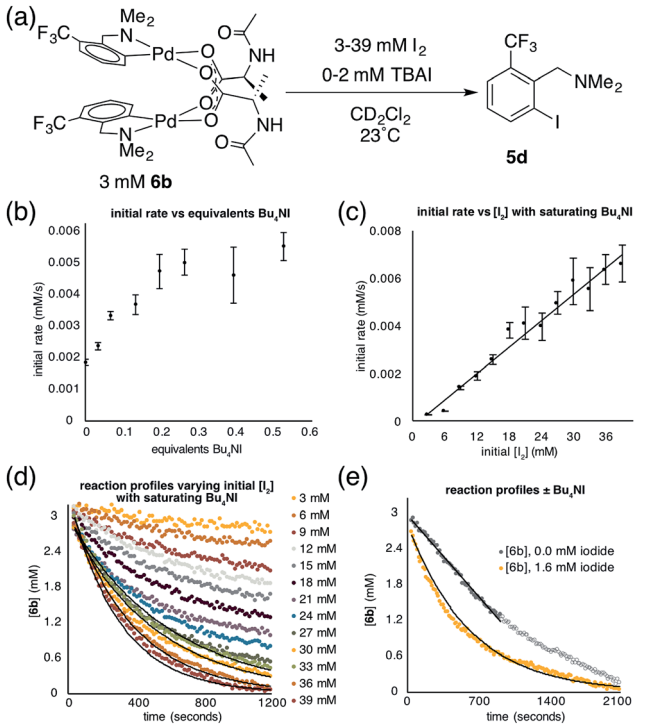

Fig. 4 (a) Iodination of cyclopalladated MPAA complex **6b**; (b) plot of initial rate of iodination of **6b** *versus* equivalents of exogenous iodide; (c) plot of initial rate of iodination of **6b** *versus* initial concentration of I_2 showing first order kinetics in I_2 under saturating Bu_4NI conditions; (d) overlaid reaction profiles of iodination of **6b** from 3–39 mM I_2 with exponential fits for pseudo-first order reactions; (e) overlaid reaction profiles of iodination of **6b** in the presence and absence of Bu_4NI with an exponential fit in the presence of Bu_4NI and a linear fit for zero order portion in the absence of Bu_4NI.

(Fig. 5a). This constitutes the first report of an MPAA-ligated palladacycle reacting to give discrete Pd(II)MPAA products.

Further investigation into the reaction of **2** with iodobenzene dichloride revealed the presence of chloride bridged dimers **16a**, and **16b**, which could result from carboxylate/chloride metathesis between **15a–b** and HCl generated *in situ* (Fig. 5a). The MPAA- and chloride-bridged di-palladium products crystallized as needles and blocks, respectively, and could be separated manually. The mono- and di-chlorinated dimers co-crystallized, however, leading to partial occupancy of the chlorinated positions in the structures shown in Fig. 5c and d. Treating **2** with excess iodobenzene dichloride led to chlorination and C–H activation of both dmba ligands and complete metathesis with chloride to give 75% **16b** and 22% **16a**, which reacted further with excess oxidant to give partial conversion to dichlorinated dmba **17** (Fig. 5b and e). The dichlorinated compound (**17**) was protonated by HCl generated *in situ* and co-crystallized as a chloro-palladate salt (Fig. 5e).

The observation of stoichiometric C–H cleavage and Pd–C functionalization starting from dimeric MPAA-bridged Pd(II) complexes raises the possibility that both C–H activation and C–H functionalization could proceed *via* dimeric complexes. We envisioned that DFT calculations could provide further insight into potential reaction mechanisms, the nuclearity of potential

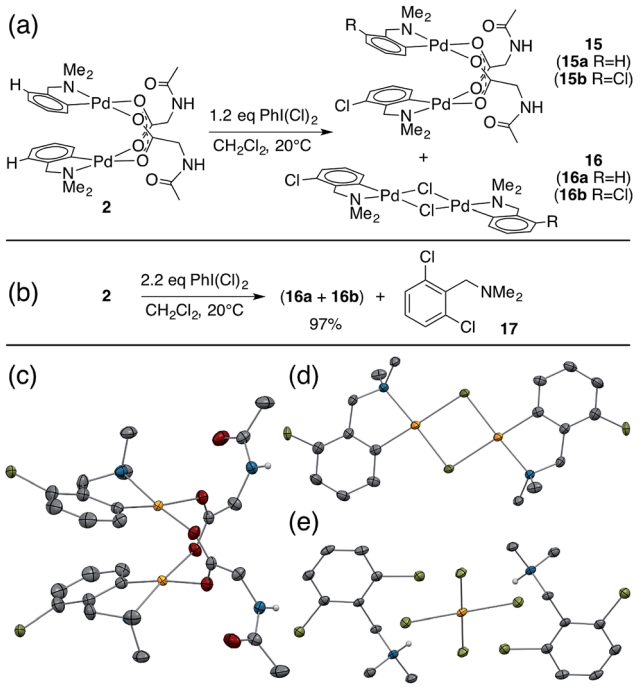

Fig. 5 (a) Sequential chlorination and C–H activation of **2**; (b) chlorination of **2** with excess iodobenzene dichloride; (c) ORTEP of co-crystallized C–H activation products **15a** and **15b**: chlorines are disordered over both positions in dimer and were refined at 50% chemical occupancy; (d) ORTEP of co-crystallized C–H activation products **16a** and **16b**: chlorines are disordered over both positions in dimer and were refined at 20% chemical occupancy; (e) ORTEP of product of dmba dichlorination (**17**) co-crystallized with chloropalladate.

intermediates (Pd(II)MPAA dimer or monomer), and factors controlling cyclopalladation and Pd–C bond functionalization for the F_3C-dmba model complexes examined.

Computational analysis of cyclopalladation of dimeric and monomeric Pd(II)/MPAA complexes

Several computational studies have established cyclopalladation pathways for monomeric Pd(II)MPAA complexes,[19–25] and we previously studied the effect of acetate-bridged dimeric Pd(II) complexes on cyclopalladation,[44] but a similar study on dimeric MPAA-bridged Pd(II) complexes has not yet been reported. Here, we investigate the mechanisms of cyclopalladation of [Pd(II) (κ-*N*–F_3C-dmba) (κ-OAc) (μ-NAc-Gly)]$_2$ (**18-D**)[69] and its monomer (**21-M**) complex (where **-D** and **-M** signify dimeric and monomeric species, respectively). The free energy surface for cyclopalladation of the lowest energy (F_3C-dmba)Pd(II)/NAc-Gly dimer and monomer systems are shown in Fig. 6 (see Fig. S2.1 and S2.2† for full energy surfaces). Prior to C–H activation, the monomer–dimer equilibrium for the (F_3C-dmba)Pd(II)/NAc-Gly system (*i.e.*, **2** (**21-M**) → **18-D**) is $\Delta G_{dimer}/\Delta H_{dimer} = -3.3/-13.5$ kcal mol^{-1}, which is much smaller than that calculated for the cyclopalladated products **6a–d**. This is attributed to the strong hydrogen bonding interaction between NAc-Gly and OAc in **21-M**. As shown in Fig. 6, the overall free energy barrier (relative to **18-D**) for the dimer pathway ($\Delta G^{\ddagger}/\Delta H^{\ddagger} = 23.2/20.3$ kcal mol^{-1}) is significantly lower than that for the monomer pathway ($\Delta G^{\ddagger}/\Delta H^{\ddagger} = 41.7/52.1$ kcal mol^{-1}). In addition, the dimer pathway has the larger driving force (again relative to the lowest reactant, **18-D**) of $\Delta G/\Delta H = -15.6/-15.5$ kcal mol^{-1} compared to the monomer pathway, which is unfavorable by $\Delta G/\Delta H = 7.2/23.9$ kcal mol^{-1}.

In both pathways, the C–H activation transition state requires an open coordination site on Pd to form the new Pd–C bond. Dissociation of one of the bridging MPAA ligands from **18-D**, which is thermodynamically unfavorable by $\Delta G/\Delta H = 20.3/18.7$ kcal mol^{-1}, leads to formation of an intermediate (**19-D**) that undergoes C–H activation with a small intrinsic barrier of 2.9 kcal mol^{-1} (**TS1-D**).[70] Therefore, for the dimer pathway, cyclopalladation occurs *via* two sequential concerted-metallation-deprotonation (CMD) steps (at the transition states **TS1-D** and **TS2-D**) with $\Delta G^{\ddagger}/\Delta H^{\ddagger} = 23.2/20.3$ and 19.0/18.3 kcal mol^{-1} energy barriers, respectively. Thus, the first cyclopalladation facilitates the second step of the reaction. On the other hand, formation of **22-M** on the monomer pathway is unfavorable by $\Delta G/\Delta H = 25.2/38.7$ kcal mol^{-1} and the intrinsic barrier for C–H activation is 16.5 kcal mol^{-1}. These results show that the dimer stabilizes the C–H activation reactant and transition state relative to the monomer. It is unlikely that only one factor is responsible for such a large difference in the dimer and monomer barriers ($\Delta\Delta G^{\ddagger} = 13.6$ kcal mol^{-1}). Instead, we attribute the acceleration in the dimer to several additive or cooperative effects including decreased *trans* effect from the bridging carboxylate to the formed Pd–C bond, intramolecular hydrogen bonding, as well as Pd–Pd and dispersive interactions between the monomer fragments.

In summary, cyclopalladation of the (F_3C-dmba)Pd(II)/MPAA dimer is calculated to be kinetically and thermodynamically favored over the monomer, indicating that the calculations generally support C–H cleavage/cyclopalladation *via* the dimer pathway. Notably, previous DFT studies of MPAA promoted C–H cleavage have evaluated energies of monomeric transitions states relative to monomeric MPAA reactants without commenting on possible dimeric pathways to C–H cleavage.[19–25] When the full potential energy surface is analyzed, as in Fig. 6, it is apparent that assessing only the intrinsic barrier to C–H cleavage (*i.e.*, **22-M** → **TS-M**, where $\Delta G^{\ddagger} = 16.5$ kcal mol^{-1}) neglects the fact the reactant in this step (**22-M**) is higher in energy than any of the intermediates or transition states on the dimer pathway. This illustrates the importance of assessing the energies of transformations involving monomeric and dimeric pathways relative to a common energetic reference when evaluating possible mechanisms for MPAA induced rate acceleration in C–H functionalization.

MPAA complexes as pre-catalysts

Based on our extensive characterization of stoichiometric C–H activation and Pd–C functionalization involving the dimeric, MPAA-bridged Pd(II) complexes outlined above, we sought to determine whether these complexes are also viable precatalysts for catalytic C–H functionalization reactions. Indeed,

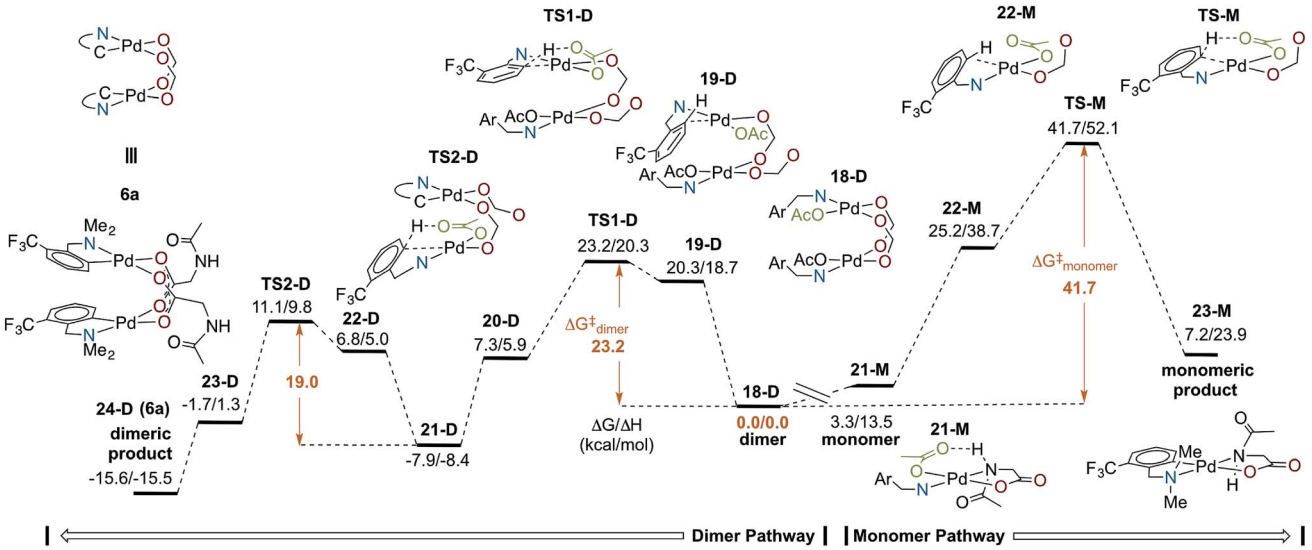

Fig. 6 Energy surfaces (Δ*G*/Δ*H*) for mononuclear and dinuclear C–H cleavage: carboxylate oxygens of NAc-Gly shown in red relevant acetate for CMD highlighted in green, and all complexes except **6a** truncated for clarity, see above **6a** for key.

alkenylation of dmba was catalyzed with the same rate whether **2** or Pd(II)/NAc-Gly was used as the precatalyst (Scheme 6). However, similar to the stoichiometric C–H activations discussed above—in which selective MPAA coordination modified the complex's secondary coordination sphere, but did not afford rate enhancements—MPAA additives also did not accelerate catalytic C–H functionalization relative to palladium(II) acetate (see Fig. S1.3–S1.5 in the ESI†). These experiments thus confirm that MPAA bridged Pd dimer complexes can generate catalysts active for C–H functionalization, but they do not shed light the nuclearity or coordination mode of the active catalyst.

On the other hand, examining the catalytic competence of isolated, structurally characterized Pd(II)MPAA complexes provides a concrete starting point for determining the nuclearity and coordination mode of intermediates in catalytic C–H functionalization reactions. Given the range of substrates and conditions used in reactions catalyzed by Pd(II)/MPAA mixtures and the potential impact of these differences on the coordination chemistry of complexes involved in catalysis, a detailed understanding of different coordination modes, such as those reported in this work, is essential. Importantly, however, characterizing the structure and reactivity of Pd(II)MPAA complexes with substrates relevant to catalysis is only a prerequisite to the loftier goal of understanding the molecular origins the rate acceleration and enantioselectivity afforded by MPAA ligands. The initial experiments summarized above using model complex **2** do not specifically implicate dimeric MPAA complexes in catalysis. On the other hand, further kinetic analysis of catalytic C–H functionalization reactions, informed by the structural characterization herein, provides a means to probe this possibility.

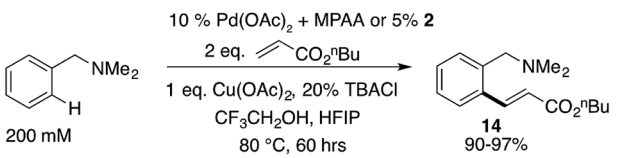

Scheme 6 Pre-catalyst **2** catalyzes olefination of dmba at the same rate as mixtures of $Pd(OAc)_2$/NAc-Gly.

Summary and conclusion

Since the discovery that MPAA ligands can accelerate and confer enantioselectivity to C–H functionalization reactions, experimental and computational studies have been conducted to understand the molecular origins of these ligand effects. Prior to our work, the structure and reactivity of discrete Pd(II)MPAA complexes remained poorly characterized. The extensive synthetic, spectroscopic, and computational studies reported herein reveal—for the first time—an unprecedented class of dimeric MPAA-bridged palladacycles that are analogous to catalytically relevant acetate bridged dimers and that form selectively from mixtures of Pd(II), MPAA, and dmba derivatives. While our work focused on dmba model complexes, MS and computational analysis of analogous complexes generated from substrates used in catalysis suggests that dimeric, MPAA-bridged palladacycles could be relevant beyond dmba substrates.

Our combined experimental and computational results show that structural features of putative Pd(II)MPAA complexes inferred from catalytic outcomes, including selective MPAA coordination and relay of stereochemistry, are observed in dmba model complexes. This finding indicates that such features do not, by themselves, necessitate κ^2-(*N*,*O*) MPAA coordination to Pd(II) during catalysis. Selective formation of dimeric, MPAA-bridged complexes from MPAA/acetate mixtures results from greater MPAA binding affinity to Pd(II) relative to acetate. Diastereotopicity in bound dmba ligands results from relay of stereochemistry from distal MPAA side chains, but

further experiments using substrates with prochiral C–H bonds will be required to determine if this phenomenon is relevant to enantioselective catalysis.

In addition to these observations, C–H activation of dmba in dimeric, MPAA-bridged complexes is calculated to be kinetically and thermodynamically favored over a monomeric pathway. Coordination of MPAA to Pd(II) in a κ^2-(*N*,*O*) fashion is also not predicted to provide access to lower barrier pathways to C–H cleavage in dmba, consistent with our experimental observation that MPAA does not influence the rate of dmba cyclopalladation. On the other hand, calculations indicate that the relative stability of different Pd(II)MPAA dimer complexes is substrate and ligand specific, such that different complexes and reaction pathways could dominate for different reactions or under different conditions.

Despite their stability with respect to carboxylate exchange and calculated monomer–dimer equilibrium, the dmba model complexes studied undergo both Pd–C functionalization and subsequent C–H cleavage reactions relevant to C–H functionalization chemistry. A detailed kinetic analysis of stoichiometric iodination revealed that MPAA-bridged palladacycles react as dimers rather than as putative monomeric intermediates. This analysis is consistent with previous calculations showing a lower barrier to iodination at a dimeric palladacycle than the corresponding monomeric complex.[71]

In addition to their stoichiometric reactivity, dimeric MPAA-bridged palladacycles are competent precatalysts in palladium catalyzed C–H functionalization. Thus, the structure and reactivity of the complexes reported herein provide a starting point for understanding the role of MPAA ligands in catalysis. For example, MPAA bridged palladacycles project hydrogen bond donors and acceptors into the secondary coordination sphere of the Pd centers and create the potential for cooperative metal–metal interactions. Given reports[72–76] of these features in catalytic mechanisms, these structural studies open the possibility of a range of additional mechanisms by which MPAA ligands might impact C–H functionalization. Alternatively, MPAA complexes could serve as stable, off-cycle catalyst reservoirs. Ongoing studies by our groups will focus on delineating possible roles of MPAA-bridged palladacycles in C–H functionalization catalysis. These fundamental studies will, in turn, provide a framework for designing improved ligands and discrete catalysts for more advanced applications.

Funding sources

This work was supported by the NSF under the CCI Center for Selective C–H Functionalization (CCHF, CHE-1205646) and by The University of Chicago Louis Block Fund for Basic Research and Advanced Study. JJG was supported by an NSF predoctoral fellowship (DGE-1144082) and by the University of Chicago Department of Chemistry. The authors gratefully acknowledge NSF MRI-R2 grant (CHE-0958205) and the use of the resources of the Cherry Emerson Center for Scientific Computation. Use of the Advanced Photon Source, an Office of Science User Facility operated for the U.S. Department of Energy (DOE) Office of Science by Argonne National Laboratory, was supported by the U.S. DOE under Contract No. DE-AC02-06-CH11357. ChemMatCARS Sector 15 is principally supported by the Divisions of Chemistry (CHE) and Materials Research (DMR), National Science Foundation, under grant number NSF/CHE-1346572.

Acknowledgements

We would like to thank CCHF members, including Jin-Quan Yu and Huw M. L. Davies, for many helpful discussions. We would also like to thank Alexander Rago for synthesizing **5a** and **9**, Alan M. Swartz for assistance acquiring mass spectra, and Zekai Lin for a preliminary solution to the structure of **15**.

References

1 S. R. Neufeldt and M. S. Sanford, *Acc. Chem. Res.*, 2012, **45**(6), 936.
2 R. G. Bergman, *Nature*, 2007, **446**, 391.
3 H. M. L. Davies and J. R. Manning, *Nature*, 2008, **451**(7177), 417.
4 H. M. L. Davies and D. Morton, *Chem. Soc. Rev.*, 2011, **40**(4), 1857.
5 J. F. Hartwig and M. A. Larsen, *ACS Cent. Sci.*, 2016, **2**(5), 281.
6 J. F. Hartwig, *J. Am. Chem. Soc.*, 2016, **138**(1), 2.
7 K. M. Engle, T.-S. Mei, M. Wasa and J.-Q. Yu, *Acc. Chem. Res.*, 2012, **45**(6), 788.
8 X. Chen, K. M. Engle, D.-H. Wang and J.-Q. Yu, *Angew. Chem., Int. Ed.*, 2009, **48**(28), 5094.
9 T. W. Lyons and M. S. Sanford, *Chem. Rev.*, 2010, **110**(2), 1147.
10 K. M. Engle, D. H. Wang and J. Q. Yu, *J. Am. Chem. Soc.*, 2010, **132**(40), 14137.
11 R. D. Baxter, D. Sale, K. M. Engle, J. Q. Yu and D. G. Blackmond, *J. Am. Chem. Soc.*, 2012, **134**(10), 4600.
12 L. Chu, K. J. Xiao and J. Q. Yu, *Science*, 2014, **346**(6208), 451.
13 X.-F. Cheng, Y. Li, Y.-M. Su, F. Yin, J.-Y. Wang, J. Sheng, H. U. Vora, X.-S. Wang and J.-Q. Yu, *J. Am. Chem. Soc.*, 2013, **135**(4), 1236.
14 L. Chu, X.-C. Wang, C. E. Moore, A. L. Rheingold and J.-Q. Yu, *J. Am. Chem. Soc.*, 2013, **135**(44), 16344.
15 K.-J. Xiao, L. Chu and J.-Q. Yu, *Angew. Chem.*, 2016, **128**(8), 2906.
16 B. N. Laforteza, K. S. L. Chan and J.-Q. Yu, *Angew. Chem.*, 2015, **127**(38), 11295.
17 B.-F. Shi, N. Maugel, Y.-H. Zhang and J.-Q. Yu, *Angew. Chem., Int. Ed.*, 2008, **47**(26), 4882.
18 K. M. Engle, *Pure Appl. Chem.*, 2016, **88**(1–2), 1.
19 B. E. Haines and D. G. Musaev, *ACS Catal.*, 2015, **5**(2), 830.
20 D. G. Musaev, T. M. Figg and A. L. Kaledin, *Chem. Soc. Rev.*, 2014, **43**(14), 5009.
21 D. G. Musaev, A. Kaledin, B. F. Shi and J. Q. Yu, *J. Am. Chem. Soc.*, 2012, **134**(3), 1690.
22 X. M. Zhong, G. J. Cheng, P. Chen, X. H. Zhang and Y. D. Wu, *Org. Lett.*, 2016, **18**(20), 5240.
23 X. F. Cong, H. R. Tang, C. Wu and H. M. Zeng, *Organometallics*, 2013, **32**(21), 6565.

24 G. J. Cheng, P. Chen, T. Y. Sun, X. H. Zhang, J. Q. Yu and Y. D. Wu, *Chem.–Eur. J.*, 2015, **21**(31), 11180.
25 G.-J. Cheng, Y.-F. Yang, P. Liu, P. Chen, T.-Y. Sun, G. Li, X. Zhang, K. N. Houk, J.-Q. Yu and Y.-D. Wu, *J. Am. Chem. Soc.*, 2014, **136**(3), 894.
26 R. D. Baxter, D. Sale, K. M. Engle, J.-Q. Yu and D. G. Blackmond, *J. Am. Chem. Soc.*, 2012, **134**(10), 4600.
27 B. Biswas, M. Sugimoto and S. Sakaki, *Organometallics*, 2000, **19**(19), 3895.
28 D. L. Davies, S. M. A. Donald and S. A. Macgregor, *J. Am. Chem. Soc.*, 2005, **127**(40), 13754.
29 S. I. Gorelsky, D. Lapointe and K. Fagnou, *J. Am. Chem. Soc.*, 2008, **130**(33), 10848.
30 L. Ackermann, *Chem. Rev.*, 2011, **111**, 1315.
31 J. C. Gaunt and B. L. Shaw, *J. Organomet. Chem.*, 1975, **102**(4), 511.
32 M. D. Diaz-de-Villegas, *J. Organomet. Chem.*, 1995, **490**, 35.
33 K. Severin, R. Bergs and W. Beck, *Angew. Chem., Int. Ed.*, 1998, **37**, 1634.
34 A. D. Ryabov, I. K. Sakodinskaya and A. K. Yatsimirsky, *J. Chem. Soc., Dalton Trans.*, 1985, **12**, 2629.
35 J. M. Thompson and R. F. Heck, *J. Org. Chem.*, 1975, **4**(18), 2667.
36 A. Van Der Ploeg, G. Van Koten and K. Vrieze, *J. Organomet. Chem.*, 1981, **222**(1), 155.
37 Geometry optimizations and frequency calculations were performed at the B3LYP-D3BJ/[6-31G(d, p) + Lanl2dz (Pd, I)] level of theory (B3LYP-D3BJ/BS1) with a polarizable continuum model (PCM) using dichloromethane to account for solvent effects. The reported energies are calculated at the B3LYP-D3BJ/[6-311+G(2d, p) + SDD (Pd, I)] level with Gibbs free energy corrections to a solution standard state of 1 M at 298.15 K with either the PCM model for methanol or dichloromethane. (See ESI† for full description of computational methodology).
38 N. R. Deprez and M. S. Sanford, *J. Am. Chem. Soc.*, 2009, **131**(31), 11234.
39 A. K. Cook and M. S. Sanford, *J. Am. Chem. Soc.*, 2015, **137**(8), 3109.
40 D. C. Powers, E. Lee, A. Ariafard, M. S. Sanford, B. F. Yates, A. J. Canty and T. Ritter, *J. Am. Chem. Soc.*, 2012, **134**(29), 12002.
41 D. C. Powers, D. Y. Xiao, M. A. L. Geibel and T. Ritter, *J. Am. Chem. Soc.*, 2010, **132**(41), 14530.
42 D. C. Powers and T. Ritter, *Nat. Chem.*, 2009, **1**(4), 302.
43 D. C. Powers, D. Benitez, E. Tkatchouk, W. A. Goddard III and T. Ritter, *J. Am. Chem. Soc.*, 2010, **132**(40), 14092.
44 B. E. Haines, J. F. Berry, J.-Q. Yu and D. G. Musaev, *ACS Catal.*, 2016, **6**(2), 829.
45 L. R. Liou, A. J. McNeil, A. Ramirez, G. E. S. Toombes, J. M. Gruver and D. B. Collum, *J. Am. Chem. Soc.*, 2008, **130**(14), 4859.
46 L. R. Liou, A. J. McNeil, G. E. S. Toombes and D. B. Collum, *J. Am. Chem. Soc.*, 2008, **130**(51), 17334.
47 E. O. Stejskal and J. E. Tanner, *J. Chem. Phys.*, 1965, **42**(1), 288.
48 P. S. Pregosin, P. G. A. Kumar and I. Fernández, *Chem. Rev.*, 2005, **105**(8), 2977.
49 C. L. Perrin and T. J. Dwyer, *Chem. Rev.*, 1990, **90**(6), 935.
50 J. S. Renny, L. L. Tomasevich, E. H. Tallmadge and D. B. Collum, *Angew. Chem., Int. Ed.*, 2013, **52**(46), 11998.
51 Mixed MPAA/OAc complex **10** is also observed in the equilibrium mixture and is shown in the ESI in Section S1.8.†
52 We also calculated the mixed intermediate species in the exchange equilibrium with Gly. The overall equilibrium is **2e** + 2 AcNH-Gly-OH → **2h** + AcOH + AcNH-Gly-OH → **2a** + 2 AcOH with $\Delta G = -2.3$ and -1.7 kcal mol^{-1} for each step. These energy values are consistent with a product distribution of **2a**/**2h**/**2e** = 89.7%/10.2%/0.1%. Thus, the DFT calculations slightly overestimate the ligand exchange equilibrium, but the trend is consistent with the experimental results.
53 D.-W. Gao, Y.-C. Shi, Q. Gu, Z.-L. Zhao and S.-L. You, *J. Am. Chem. Soc.*, 2013, **135**(1), 86.
54 C. Pi, Y. Li, X. Cui, H. Zhang, Y. Han and Y. Wu, *Chem. Sci.*, 2013, **4**(6), 2675.
55 V. I. Sokolov, L. L. Troitskaya and O. A. Reutov, *J. Organomet. Chem.*, 1979, **182**(4), 537.
56 V. I. Sokolov, L. L. Troitskaya and N. S. Khrushchova, *J. Organomet. Chem.*, 1983, **250**(1), 439.
57 N. Dendele, F. Bisaro, A.-C. Gaumont, S. Perrio and C. J. Richards, *Chem. Commun.*, 2012, **48**(14), 1991.
58 M. E. Günay and C. J. Richards, *Organometallics*, 2009, **28**(19), 5833.
59 L. V. Desai, K. J. Stowers and M. S. Sanford, *J. Am. Chem. Soc.*, 2008, **130**(40), 13285.
60 A. J. Canty, N. J. Minchin, B. W. Skelton and A. H. White, *J. Chem. Soc., Dalton Trans.*, 1986, **10**, 2205.
61 T. K. Hollis and L. E. Overman, *Tetrahedron Lett.*, 1997, **38**(51), 8837.
62 The observed ions are represented as carboxylate bridged dimers based on our characterization of **1a** and **2a–e**, as well as reported acetate and trifluoroacetate bridged analogues of **3c** and **3b**, though further structural work would be required to rigorously establish the proposed connectivity.
63 I. Y. Yakushev, A. E. Gekhman and A. P. Klyagina, *Russ. J. Coord. Chem.*, 2016, **42**(9), 604.
64 Y. Fuchita, *Inorg. Chem.*, 1982, **20**(12), 4316.
65 B.-F. Shi, Y.-H. Zhang, J. K. Lam, D.-H. Wang and J.-Q. Yu, *J. Am. Chem. Soc.*, 2010, **132**(2), 460.
66 R.-Y. Tang, G. Li and J.-Q. Yu, *Nature*, 2014, **507**(7491), 215.
67 X.-C. Wang, Y. Hu, S. Bonacorsi, Y. Hong, R. Burrell and J.-Q. Yu, *J. Am. Chem. Soc.*, 2013, **135**(28), 10326.
68 Bromination of **6b** proceeds orders of magnitude faster than iodination, consistent with calculated barriers to palladacycle halogenation: see Fig. S1.2 in the ESI.†
69 J. Vicente, I. Saura-Llamas, M. G. Palin, P. G. Jones and M. C. Ramírez de Arellano, *Organometallics*, 1997, **16**(5), 826.
70 It should be noted that the lowest energy dimer pathway for C–H activation calculated here is different than the pathway

reported by us in ref. 44. See Fig. S2.1† for a comparison of these pathways.
71 B. E. Haines, H. Xu, P. Verma, X.-C. Wang, J.-Q. Yu and D. G. Musaev, *J. Am. Chem. Soc.*, 2015, **137**(28), 9022.
72 D. C. Powers and T. Ritter, *Acc. Chem. Res.*, 2012, **45**(6), 840.
73 R. C. Cammarota and C. C. Lu, *J. Am. Chem. Soc.*, 2015, **137**(39), 12486.
74 R. B. Siedschlag, V. Bernales, K. D. Vogiatzis, N. Planas, L. J. Clouston, E. Bill, L. Gagliardi and C. C. Lu, *J. Am. Chem. Soc.*, 2015, 150323142749002.
75 A. S. Borovik, *Acc. Chem. Res.*, 2005, **38**(1), 54.
76 S. A. Cook and A. S. Borovik, *Acc. Chem. Res.*, 2015, **48**(8), 2407.